Microfluidics and Nanofluidics (2020) 24:38
https://doi.org/10.1007/s10404-020-02345-3

RESEARCH PAPER

Consecutive synthesis of gold nanobipyramids with controllable morphologies using a microfluidic platform

Ziran Ye[1,3] · Ke Wang[1] · Meinan Lou[1] · Xiqian Jia[1] · Fengyun Xu[1] · Gaoxiang Ye[2]

Received: 10 March 2020 / Accepted: 15 April 2020 / Published online: 25 April 2020

Abstract

We report a microfluidic chip designed and fabricated for the consecutive synthesis of gold nanobipyramids (Au NBPs) with controllable morphology. The seed-mediated method is employed to synthesize Au NBPs in an S-shaped micromixer. Under sufficient mixing and precise flow rate control of various reactants during microfluidic synthesis, Au NBPs with various aspect ratios can be obtained through this microfluidic platform. The dependence of reactant concentration on the morphology of synthesized Au NBPs is studied by changing the flow rate of silver nitrate ($AgNO_3$), ascorbic acid (AA) and gold seed in microchannel respectively, analytical simulation is performed to validate the control mechanism during Au NBPs synthesis in a microchannel.

Keywords Microfluidics · Lab-on-a-chip · Consecutive · Gold nanobipyramid · Synthesis

1 Introduction

In recent years, synthesis of anisotropic nanoparticles has attracted considerable attention in biomedicine owing to their unique properties in spectroscopy, photoelectricity, catalysis sensing and drug delivery (Weissleder et al. 2014; Pappas et al. 2007; Cong and Porco 2012; Nath and Chilkoti 2002; Gelperina et al. 2005). The substantial potential applications mainly lie in their intriguing localized surface plasmon resonance (LSPR) characteristics, in which anisotropic metal nanoparticles (rods, bipyramids, and decahedra) exhibit two surface plasma resonances corresponding to both transverse and longitudinal modes thus own more prominent advantages (Qi et al. 2016). Comparing with the LSPR properties of Au nanorods, the sharp edge structure of Au NBPs is more sensitive to local changes in the dielectric environment and has greater enhancement of localized electric field (Navarro et al. 2012; Li et al. 2015). Substantial efforts have been subsequently made to prepare anisotropic metal nanoparticles (Chateau et al. 2015; Huang et al. 2009; Kou et al. 2006), among which seed-mediated method is one of the most commonly used and well-established methods to form cores and further increase in particle size to form various anisotropic metal nanoparticles (Jana et al. 2001, 2002). In general, the seed-mediating method has a two-step synthesis process, including the formation and activation of precursor solution, followed by intensive mixing with gold seeds solution to generate the nanoparticles (Jana et al. 2001). Although extensive progress has been made in Au NBPs synthesis with a high degree of monodispersity, the synthesis of Au NBPs with different sizes and aspect ratios still requires a cumbersome adjustment process (Kou et al. 2007). In conventional bulk synthesis, it is difficult to control the thermodynamic and kinetic factors in the synthesis of nanoparticles (Ma and Li 2018). Besides, it takes time and energy during the synthesis process and consumes reagents to screen the controlling factors to prepare gold nanoparticles with various morphologies (Thiele et al. 2016). The tedious synthetic process of growth solution and the structural instability of gold seeds result in the limitation of the yield, shape and reproducibility of Au NBPs, which has greatly hindered their potential for practical applications. Therefore, it is of great importance to develop a synthetic

✉ Ziran Ye
yeziran@zjut.edu.cn

[1] Department of Applied Physics, College of Science, Zhejiang University of Technology, Hangzhou, China

[2] Department of Physics, Zhejiang University, Hangzhou, China

[3] Center for Optics and Optoelectronics Research (COOR), Collaborative Innovation Center for Information Technology in Biological and Medical Physics, College of Science, Zhejiang University of Technology, Hangzhou, China

process to achieve precise control in the morphology and size of Au NBPs with high yield and reproducibility.

Microfluidics is a powerful tool for manipulating fluids in the miniaturized device due to their precise control, high throughput, rapid mass and heat transfer (Whitesides 2006; Ren et al. 2013; Li et al. 2017; Chen et al. 2019). The continuous-flow microfluidic systems with large reaction interfaces and high sensitivity provide promising modulation in nanoparticle synthesis, especially in some critical synthetic stages such as nucleation, growth and reacting conditions, thus can serve as a well-controlled microenvironment for the synthesis of nanoparticles with desired size and morphology (Ma et al. 2019). Although substantial research efforts have been devoted to the microfluidic synthesis of anisotropic nanoparticles (Duraiswamy and Khan 2009; Boleininger et al. 2006; Uson et al. 2016), the precise control of Au NBPs synthesis with optimized morphology, size distribution and reproducibility has been rarely reported.

In this paper, a microfluidic platform is designed to investigate the consecutive and controllable synthesis of gold nanoparticles with various morphologies. An improved seed-mediated method was employed for the Au NBPs synthesis in an S-shaped micromixer. Our microfluidic chip can be divided into two parts, in which the gold precursor solution successively forms in one part, and the Au(III) solution is gradually reduced to Au(I) by ascorbic acid. Afterwards, gold seeds are mixed with the precursor solution in the other part (Huang et al. 2007). Through syringe pumps at each inlet of microchannel, flow rates of synthetic reactants including $AgNO_3$, AA and gold seeds can be adjusted instantaneously during the synthesis process. We investigate and optimize the flow rate of each reactant to realize complete mixing and accurate morphology control of synthesized Au NBPs in a microchannel.

2 Materials and methods

2.1 Chemicals

Polydimethylsiloxane (PDMS) was purchased from Dow Corning Corporation (State of Michigan, America). Hexadecyl trimethyl ammonium bromide (CTAB, 99%) and cetyltrimethylammonium chloride (CTAC, 99%) were purchased from Macklin. Gold chloride trihydrate ($HAuCl_4$, ≥ 99.9%), $AgNO_3$ (99.8%), ascorbic acid (AA, > 99.0%), potassium tetrachloropalladate (K_2PdCl_4, ≥ 99.95%) and sodium borohydride ($NaBH_4$, 98%) were purchased from Aladdin. All chemicals were used as received and deionized (DI) water (18.2 MΩ cm) was used for the preparation of solutions throughout the experiments.

2.2 Fabrication of the microfluidic chip

A schematic illustration of the fabrication process of the microfluidic chip is depicted in Fig. 1. A dark-field lithography mask was designed in AUTOCAD 2015 and printed in advance, and the photolithography for the fabrication of microfluidic chip was performed in a clean room. A 100 μm layer of SU-8 2075 photoresist (Micro-Chem) was

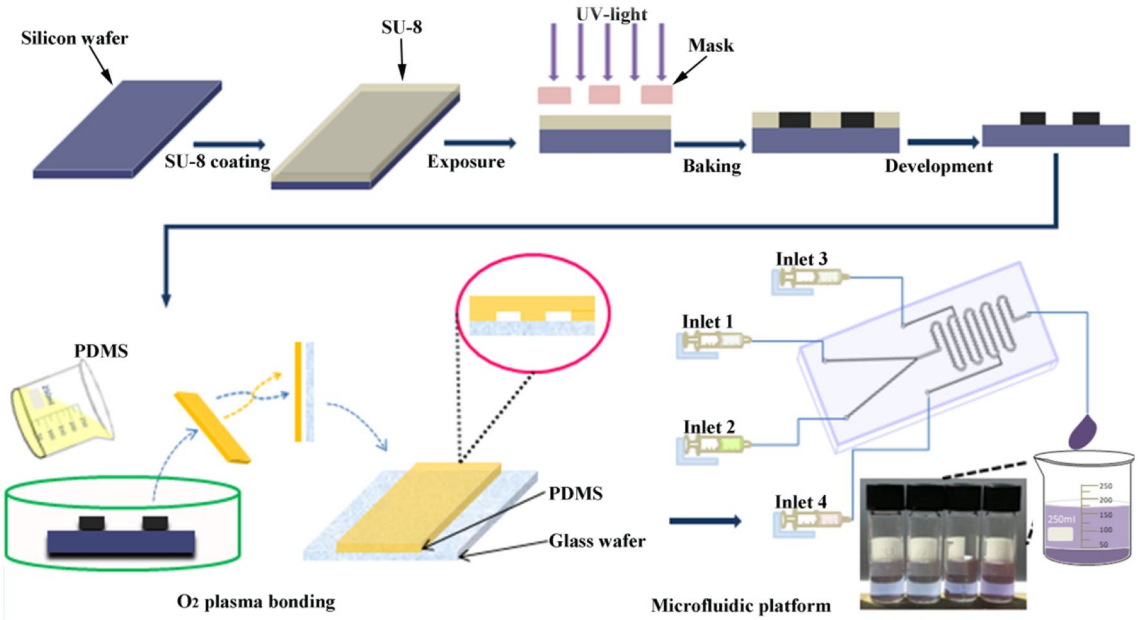

Fig. 1 Schematic illustration of microfluidic chip fabrication for Au NBPs synthesis. The inset exhibits the photograph of prepared Au NBPs solution synthesized with various flow rates of gold seed range from 40 to 160 μl/min (from left to right) respectively

spin-coated onto a cleaned 4-inch silicon wafer uniformly, the wafer was then prebaked at 65 °C for 5 min and 90 °C for 10 min, followed by UV light exposure through the mask via a mask aligner (MJB4, Suss Microtech). The silicon wafer was hard-baked for 1 min at 90 °C, and SU-8 developer was then used to remove surplus cured SU-8. For the fabrication of the microfluidic chips, a 10:1 mixture of base polymer PDMS and the curing agent was poured over the mask placed in a petri dish and then degassed in vacuum until no bubbles can be observed. After curing for 1.5 h in the oven at 90 °C, the cured PDMS was peeled off and cut into desired shapes for use. Well-defined through-holes were drilled on the PDMS layer for tubing connection. Finally, oxygen plasma was used to bond the PDMS and the glass wafers to obtain a completed microfluidic chip in which S-shaped microchannels with a depth of 100 um and width of 200 um were prepared.

2.3 Synthesis of gold seeds solution

In our experiment, gold seeds were prepared by reducing $HAuCl_4$ with $NaBH_4$, following the method developed by Ana Sánchez-Iglesias et al. (Sánchez-Iglesias et al. 2016; Fang et al. 2016). Initial gold seeds were prepared by adding $HAuCl_4$ (50 µl, 50 mM) to an aqueous solution which contains CTAC (10 ml, 100 mM), then a freshly prepared ice-cold $NaBH_4$ (60 µl, 100 mM) solution was added. Under vigorous stirring at room temperature, the aqueous mixture changes from yellow to brownish, indicating the production of gold seeds. After that, the solution was heated in a water bath at 80 ℃ for 90 min, and the solution further changes from brown to claret-red. K_2PdCl_4 (25 µl, 50 mM) was added to 10 ml as-prepared gold seeds and the solution was kept at 40 ℃ for 15 min to allow the complexation of palladium salt with CTAB. AA (250 µl, 100 mM) was then added into the solution and kept at room temperature for 12 h.

2.4 On-chip Au NBPs synthesis

As illustrated in Fig. 1, the as-fabricated S-shaped micromixer was utilized to consecutively adjust parameters in the gold nanoparticles synthesis. Polytetrafluoroethylene (PTFE) tubes were utilized for the connection between inlets of the microfluidic chip and syringe pumps for reactants injection. The process of Au NBPs synthesis in the microfluidic chip can be divided into two parts, precursor formation part and gold seed mixing part, respectively. For the precursor formation part, a mixed solution with 200 mM CTAB, 0.25 mM $HAuCl_4$, and 200 mM HCl was introduced into microchannel through inlet 1 (S_1); 1 mM $AgNO_3$, 4 mM AA and 0.25 µM gold seeds were injected through inlet 2 (S_2), inlet 3 (S_3), inlet 4 (S_4), respectively. In this part, the precursor solution at S1 was mixed with $AgNO_3$ at S2 firstly, followed by consecutive mixing with AA at S3, after which the solution changed from orange into colorless and transparent, indicating that Au(III) has been reduced to Au(I) by AA. In the second part, the precursor solution was further mixed with gold seed solution at S4. After sufficient mixing in the S-shaped micromixer, the fully mixed solution was collected through the outlet and then kept undisturbed for 2 h to generate Au NBPs.

2.5 Characterization

The morphologies of synthesized gold nanoparticles were characterized using a scanning electron microscopy (SEM, Zeiss Supratm 55) which was operated at an acceleration voltage of 15 kV. In a typical sample preparation, a drop of the solution with synthesized nanoparticles was added to a 1 cm^2 polished silicon wafers and then dried naturally at room temperature. The ultraviolet–visible light (UV–vis) absorption spectroscopy was detected using an assembled UV–vis spectrophotometer.

3 Results and discussion

During our experiments, the flow rates of reactants at each inlet of the micromixer can be conveniently adjusted through syringe pumps to obtain the desired morphology of Au NBPs. As exhibited in Table 1 below, we set the flow rate of $AgNO_3$ between 0 µl/min and 160 µl/min, AA from 60 µl/min to 160 µl/min, gold seed between 40 µl/min and 160 µl/min. The total estimated synthetic flow rate during the synthesis process ranges from 360 µl/min to 520 µl/min. By varying the flow rates of $AgNO_3$, AA and gold seeds at

Table 1 Flow rates of reactants at each inlet of the microchannel (µl/min)

Condition	No	S1($HAuCl_4$, CTAB) HCL)	S2($AgNO_3$)	S3(AA)	S4(Seed)
$AgNO_3$	1	200	0	80	80
	2	200	40	80	80
	3	200	80	80	80
	4	200	160	80	80
Seed	1	200	80	80	40
	2	200	80	80	80
	3	200	80	80	120
	4	200	80	80	160
AA	1	200	80	60	80
	2	200	80	80	80
	3	200	80	120	80
	4	200	80	160	80

S1, S2, S3 separately, the dependence of the concentration of each reactant on the morphology of synthesized Au NBPs can be systematically investigated.

3.1 Au NBPs morphology control by changing $AgNO_3$ flow rate

Silver ions are indispensable in the formation of anisotropic gold nanoparticles, which has been discussed in the underpotential deposition theory (Liu and Guyot-Sionnest 2005). Defect-free deposition is a unique property of Ag(I) assisted growth, it may allow the gold atoms to be deposited at the most energy favorable place and create no defect (Liu and Guyot-Sionnest 2005). With the aid of Ag(I), the deposition of gold atoms on the surface of the seed produces little or no observable stacking faults, thus preserve the original twin structure (Liu and Guyot-Sionnest 2005). In our experiments, the flow rate of $AgNO_3$ in micromixer was adjusted from 0 to 160 µL/min, and the corresponding SEM images of synthesized Au nanoparticles are shown in Fig. 2a, b, d, e. In Fig. 2a, spherical Au nanoparticles with a mean diameter of ~ 56 nm can be obtained in the absence of $AgNO_3$, indicating the isotropic growth of gold seeds without $AgNO_3$. The spherical Au nanoparticles gradually turn in to Au NBPs with well-defined facets when the flow rate of $AgNO_3$ increases, as observed in Fig. 2b, d, e. Besides, the sizes of synthesized Au NBPs are obtained by measurements of 100 random Au NBPs for each sample according to SEM images. The results indicate that the average length of Au NBPs gradually increases from 134 to 145 nm, and the width increases from 44 to 48 nm with the increasing flow rate of $AgNO_3$. Figure 2c exhibits the dependence of the $AgNO_3$ flow rate on the aspect ratio of the synthesized Au NBPs. Since the length and width of Au NBPs both increase slightly as the $AgNO_3$ flow rate increases, the aspect ratio of Au NBPs almost keeps unchanged under the presence of $AgNO_3$. Figure 2f shows the corresponding UV–vis absorption spectra of synthesized Au NBPs with $AgNO_3$ flow rate ranges from 40 to 160 µL/min. As shown in the spectrum, only one absorption peak at 550 nm is detected without $AgNO_3$, the longitudinal resonance peak appears with the presence of $AgNO_3$. Besides, the intensity of the longitudinal resonance peak keeps almost unchanged when $AgNO_3$ flow rate increases from 40 to 80 µL/min, with the peak position slightly red-shifted. As the $AgNO_3$ flow rate further increases from 80 to 160 µL/min, however, the longitudinal absorption peak intensity has a significant decrease with an unchanged location. These experimental results indicate that the $AgNO_3$ flow rate range of 40 to 80 µL/min is beneficial to the increase of the yield of Au NBPs. This conclusion is in accordance with previous work in which optimal amount of $AgNO_3$ has a significant effect on the growth and yield of Au NBPs, lower or no LSPR band of Au NBPs can be observed and the yield was not improved with higher or lower concentration of $AgNO_3$ (Qi et al. 2016).

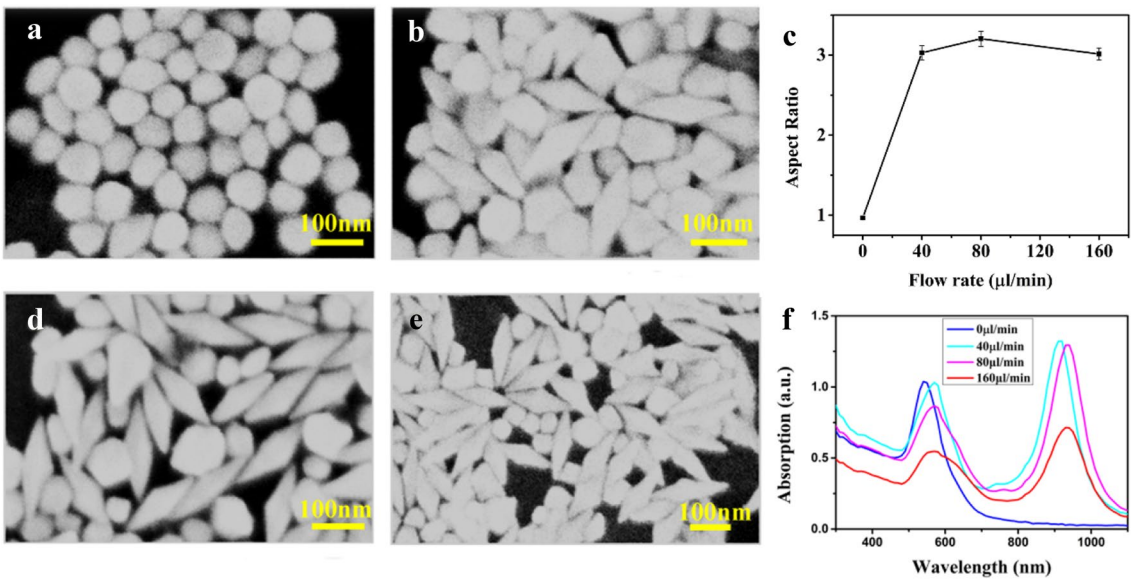

Fig. 2 SEM images of synthesized Au nanoparticles with various flow rates of $AgNO_3$: (**a**) 0µL/min, (**b**) 40 µL/min, (**d**) 80 µL/min, (**e**) 160 µL/min. (**c**) Aspect ratio of synthesized Au nanoparticles with various flow rates of $AgNO_3$. (**f**) UV–vis absorption spectra of synthesized Au nanoparticles with various flow rates of $AgNO_3$

3.2 Au NBPs morphology control by changing Gold seed flow rate

The amount of gold seeds plays a crucial role in the seed-mediated method to synthesize Au NBPs. In our experiment, the flow rate dependence of gold seeds on the microfluidic synthesis of Au NBPs is studied in a quantitative manner. As shown in SEM images in Fig. 3a, b, d, e, with the increasing flow rate of gold seeds, the length of synthesized Au NBPs decreases from 157 to 104 nm, and the width of synthesized Au NBPs decreases from 53 to 34 nm, respectively. Besides, according to the SEM images, the aspect ratio of Au NBPs also decreases continuously as the flow rate of gold seeds increases, as shown in Fig. 3c. Figure 3f shows the UV–vis absorption spectrum of the microfluidic synthetic Au NBPs with gold seed flow rate ranges from 40 to160 µL/min, in which the spectrum exhibits a significant blue shift when the flow rate of gold seed increases and the longitudinal absorption peak intensity increases successively. The decrease in length, width and aspect ratio of Au NBPs may be due to that as the flow rate of gold seed increases, the competition of gold seed becomes fiercer, resulting in the decreased gold ions occupied by each gold seed. As the flow rate of gold seeds further increases, the gold ions deposited are not enough to the synchronous growth of width and length of Au NBPs. Since high mole ratio of Au(III)/Au(seed) is more favorable for longitudinal ({100} facet) growth (Sánchez-Iglesias et al. 2016), the decreasing Au(III)/Au(seed) ratio preferably facilitates the lateral growth, resulting in the reduced aspect ratio of synthesized Au NBPs.

3.3 Au NBPs morphology control by changing AA flow rate

AA is a necessary condition for the formation of a precursor solution that can be used to reduce Au(III) to Au(I) (Ma and Li 2018). In general, the amount of AA is insufficiency to reduce all Au(III), thus the reaction rate is directly related to the AA concentration (Ma and Li 2018). Under this kinetic control, the influence of AA flow rate on the synthesis of Au NBPs is investigated. SEM images in Fig. 4a, b, d, e show that when the AA flow rate increases from 60 to 160 µL/min, the length of synthesized Au NBPs decreases from 160 to 79 nm, and the width decreases from 62 to 38 nm, respectively. Besides, large amounts of spherical and square by-products exist at the AA flow rate of 60 µL/min as shown in Fig. 4a. However, the amounts of by-products decrease significantly as the AA flow rate further increases to 120 µL/min as shown in Fig. 4b, d. The longitudinal absorption peak of the UV–vis absorption spectrum appears as a blue shift in Fig. 4f under this AA flow rate range, indicating the optimized condition for sufficient yield of Au NBPs.

In addition, Fig. 4c shows the relationship of the AA flow rate and aspect ratio of synthesized Au nanoparticles. There is a continuous increase in the aspect ratio of Au NBPs as the AA flow rate increases from 60 to 120 µL/min. This may be due to that the increased flow rate of AA facilitates the reduction of Au(III) to Au(I), the increasing ratio of Au(I)/Au(seed) results in the increased aspect ratio of Au NBPs. However, a decrease dramatically occurs as the AA flow rate further increases to 160 µL/min. The possible cause is that when adding too much reducing agent, the Reynolds number

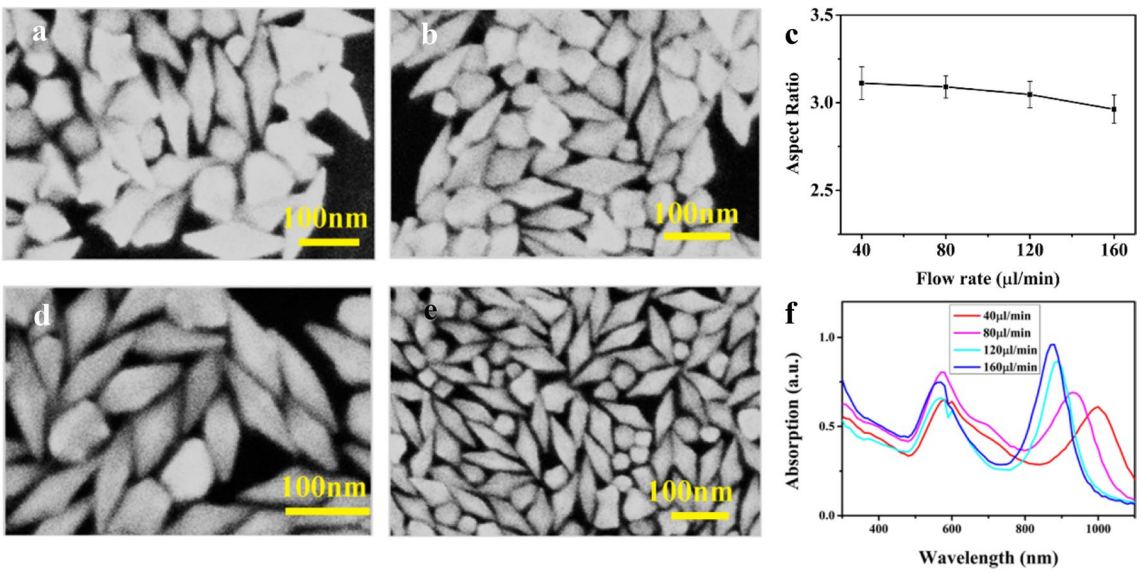

Fig. 3 SEM images of synthesized Au nanoparticles with various flow rates of gold seeds: (**a**) 40 µL/min, (**b**) 80 µL/min, (**d**) 120 µL/min, (**e**) 160 µL/min. **c** Aspect ratio of synthesized Au nanoparticles with various flow rates of gold seeds. **f** UV–vis absorption spectra of synthesized Au nanoparticles with various flow rates of gold seeds

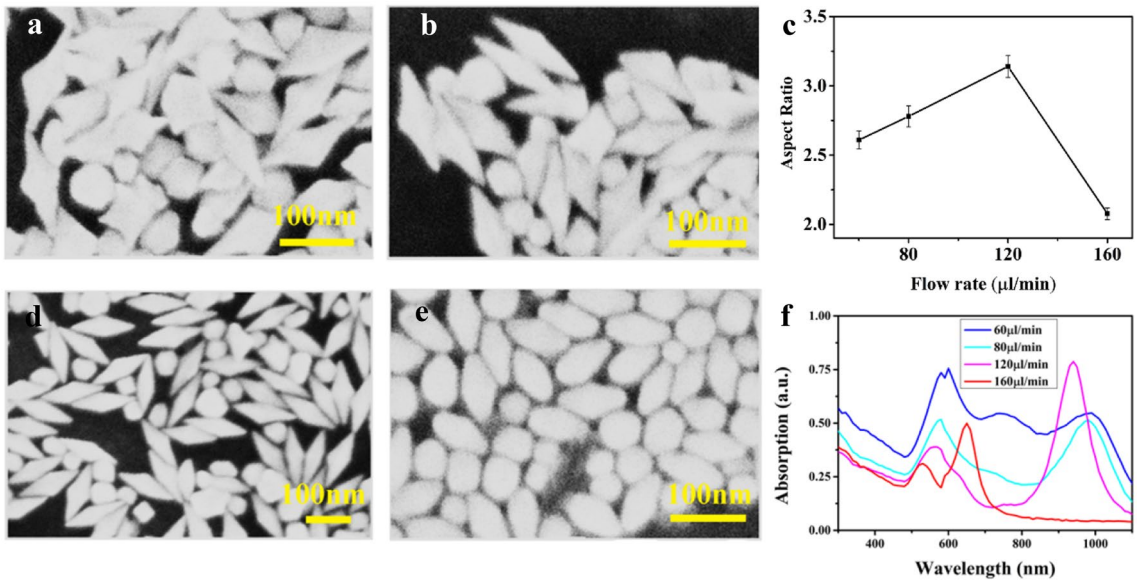

Fig. 4 SEM images of synthesized Au nanoparticles with various flow rates of AA: (**a**) 60 μL/min, (**b**) 80 μL/min, (**d**) 120 μL/min, (**e**) 160 μL/min. (**c**) Aspect ratio of synthesized Au nanoparticles with various flow rates of AA. **f** UV–vis absorption spectra of synthesized Au nanoparticles with various flow rates of AA

in microchannel increases with AA flow rate, resulting in the more turbulent flow of reactants. Thus, the excessive supply of Au(I) is available to the seeds quickly which promote the choice of absorption in all directions on the seeds, leading to the decreasing of aspect ratios of Au NBPs. In addition, the excessive Au(I) resulted in the generation of new gold nanoparticles (Qi et al. 2016; Li et al. 2013) and form more by-products (Qi et al. 2016). It should be noted that, when the AA flow rate reaches 160 μL/min, although the aspect ratio is significantly reduced, the width is decreasing as well, leading to the continuing blue shift in the absorption spectrum (Lohse et al. 2013).

3.4 COMSOL simulation for the mixing effect in microchannel

The sufficient mixing of various reactants plays a crucial role in the Au NBPs synthesis. To further evaluate the mixing performance in the microchannel, numerical simulations were also performed by Comsol Multiphysics (COMSOL 5.4) to validate the mechanism and effectiveness of our micromixer during the Au NBPs synthesis.

For the simulational model, we build a three-dimensional microchannel under the microfluidic module in Comsol at first and select the fluid flow as laminar flow. The width of the microchannel is 200 μm, the depth is 100 μm, and the total length is about 9 cm, all dimensions of the microchannel is in accordance with the actual design in the microfluidic chip. The boundary conditions and fluid properties are set, with the fluid density of 1000 kg/m^3, the diffusion coefficient of 10^{-9} m^2/s, inlet pressure of 7500 Pa, and dynamic viscosity of $1*10^{-3}$Pa s.

The concentration distribution of various reactants flowing through the S-shaped microchannel is presented in Fig. 4a (not drawn to scale), in which a diffusion mixing layer was developed as the fluids with different initial concentrations were brought into contact. By comparing the concentration variation at the interface of different reactants in the microchannel, it can be seen that the width of this mixing layer increased along the flow direction in the microchannel, indicating the enhanced microfluidic mixing effect. Velocity distribution and pressure distribution inside microchannel are exhibited in Fig. 5b, c respectively, from which we can see that the nonuniform velocity and pressure distribution occur at the curved section of the microchannel, resulting in the instability and variation of fluidic concentration. These results unambiguously indicate the evident enhancement on microfluidic mixing and thus validate the benefit of the S-shaped micromixer for Au NBPs synthesis in the microchannel.

From both the experimental results and analytical simulation we can obtain the general relationship between the Au NBPs synthesis and flow rates of various reactants in the microchannel, which can be mainly attributed to the enhanced mixing effect caused by S-shaped micromixer to promote the synthetic process. In addition, these experimental results can be implemented to further study the influence of each parameter, and optimize the synthetic condition of Au NBPs in the microchannel. The design of our microfluidic chips is in accordance with the experimental

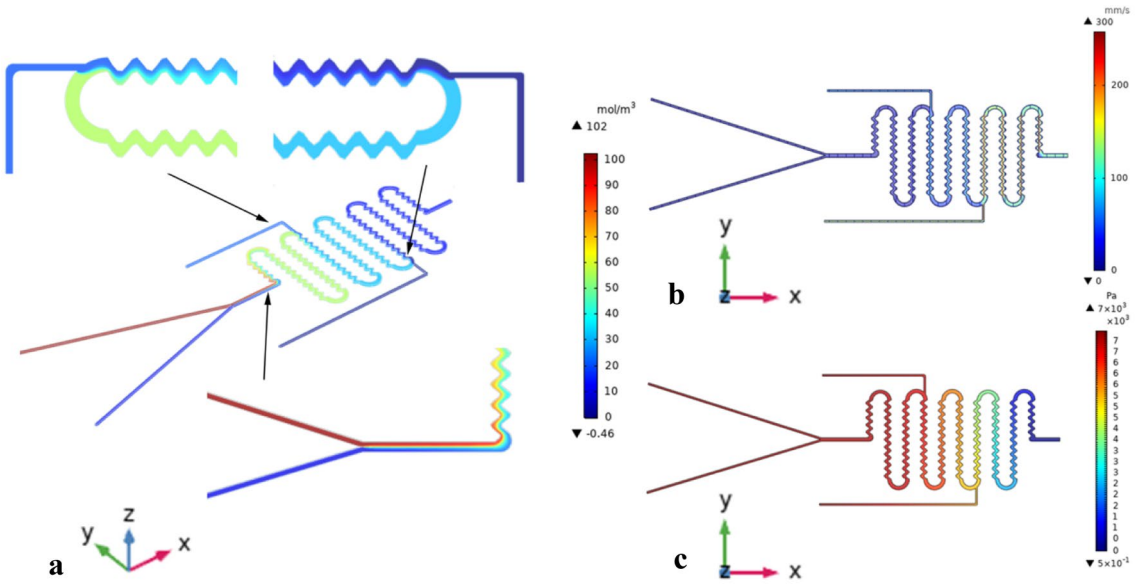

Fig. 5 Simulation results of (**a**) concentration distribution of various reactants, (**b**) velocity distribution, (**c**) pressure distribution inside the S-shaped micromixer (not drawn to scale)

steps of the improved seed-mediated method in the beakers, the three mixing junctions in microchannels can ensure the addition order of various reactants for Au NBPs synthesis. With respect to the traditional solution-based synthesis in beakers which will be influenced by surrounding conditions, this on-chip microfluidic platform can provide a controllable environment with high stability and reproducibility in the synthesis process, as well as the instantaneous transformation between spherical Au nanoparticles and Au NBPs, which greatly avoids tedious experimental operation when preparing these two kinds of nanoparticles at the same time. Besides, this microfluidic synthesis can greatly save time needed for reagent implementation and adjustment, as well as promote the ability to feedback and improvement.

It is worth mentioning that, although the Au NBPs were successfully synthesized in the microchannel, it was found that spherical nanoparticles inevitably appeared as shown in the SEM images. Therefore, purification methods (Li et al. 2015) may be utilized to further screen out Au NBPs.

4 Conclusion

In summary, this work proposes an effective method for consecutive synthesis of Au NBPs with controllable morphologies via a microfluidic platform. The improved seed-mediated method was utilized, Au NBPs with various sizes and aspect ratios can be synthesized by adjusting the flow rates of various reactants in an S-shaped microchannel. The microfluidic mixer has a prominent mixing performance, as well as the capability of fast and continuous parameter adjustment, which is crucial and convenient for the controllable synthesis of Au NBPs with optimized morphology. The mixing effect in the microchannel was validated by the simulation method, and the dependence of flow rates of reactants in each inlet of microchannel was systematically studied. These experimental results provide a feasible and effective approach for controllable synthesis of Au NBPs in the microchannel, which shows the potential to control the morphology of various anisotropic nanoparticles in more sophisticated devices and miniaturized analytical systems.

Acknowledgements We thank Dr. Xiuqing Gong for technical assistance. The research was supported by the National Natural Science Foundation of China (Grant No. 11604295, Grant No. 61705197, Grant No. 21775101) and Shanghai Pujiang Program (17PJ1402800).

References

Boleininger J, Kurz A, Reuss V, Sonnichsen C (2006) Microfluidic continuous flow synthesis of rod-shaped gold and silver nanocrystals. Phys Chem Chem Phys 8:3824–3827

Chen G, Ji B, Gao Y, Wang C, Wu J, Zhou B, Wen W (2019) Towards the rapid and efficient mixing on 'open-surface' droplet-based microfluidics via magnetic actuation. Sensor Actuat B-Chem 286:181–190

Chateau D, Liotta A, Vadcard F, Navarro JRG, Chaput F, Lermé J, Lerouge F, Parola S (2015) From Au NBPs to nanojavelins for a precise tuning of the plasmon resonance to the infrared wavelengths: experimental and theoretical aspects. Nanoscale 7:1934–1943

Cong H, Porco JA Jr (2012) Chemical synthesis of complex molecules using nanoparticle catalysis. ACS Catal 2:65–70

Duraiswamy S, Khan SA (2009) Droplet-based microfluidic synthesis of anisotropic metal nanocrystals. Small 5:2828–2834

Fang C, Zhao G, Xiao Y, Zhao J, Zhang ZJ, Geng BY (2016) Facile growth of high-yield Au NBPs induced by chloroplatinic acid for high refractive index sensing properties. Sci Rep 6:36706

Gelperina S, Kisich K, Iseman MD, Heifets L (2005) The potential advantages of nanoparticle drug delivery systems in chemotherapy of tuberculosis. Am J Resp Crit Care 172:1487–1490

Huang X, Neretina S, El-Sayed MA (2009) Gold nanorods: from synthesis and properties to biological and biomedical applications. Adv Mater 21:4880–4910

Huang XH, Jain PK, El-Sayed IH, El-Sayed MA (2007) Gold nanoparticles: interesting optical properties and recent applications in cancer diagnostics and therapy. Nanomedicine 2:681–693

Jana NR, Gearheart L, Murphy CJ (2001) Seed-mediated growth approach for shape-controlled synthesis of spheroidal and rod-like gold nanoparticles using a surfactant template. Adv Mater 13:1389–1393

Jana NR, Gearheart L, Obare SO, Murphy CJ (2002) Anisotropic chemical reactivity of gold spheroids and nanorods. Langmuir 18:922–927

Kou XS, Zhang S, Tsung CK, Yeung MH, Shi QH, Stucky GD, Sun LD, Wang JF, Yan CH (2006) Growth of gold nanorods and bipyramids using CTEAB surfactant. J Phys Chem B 110:16377–16383

Kou XS, Ni WH, Tsung CK, Chan K, Lin H-Q, Stucky GD, Wang JF (2007) Growth of gold bipyramids with improved yield and their curvature-directed oxidation. Small 3:2103–2113

Li S, Zeng M, Gaule T, McPherson MJ, Meldrum FC (2017) Passive pico-injection enables controlled crystallization in a droplet microfluidic device. Small 13:1702154

Li Q, Zhuo XL, Li S, Ruan QF, Xu QH, Wang JF (2015) Production of monodisperse Au NBPs with number percentages approaching 100% and evaluation of their plasmonic properties. Adv Optical Mater 3:801–812

Li X, Yang Y, Zhou G, Han S, Wang W, Zhang L, Chen W, Zou C, Huang SM (2013) The unusual effect of $AgNO_3$ on the growth of Au nanostructures and their catalytic performance. Nanoscale 5:4976–4985

Liu MZ, Guyot-Sionnest P (2005) Mechanism of silver (I)-assisted growth of gold nanorods and bipyramids. J Phys Chem B 109:22192–22200

Lohse SE, Eller JR, Sivapalan ST, Plews MR, Murphy CJ (2013) A simple millifluidic benchtop reactor system for the high-throughput synthesis and functionalization of gold nanoparticles with different sizes and shapes. ACS Nano 7:4135–4150

Ma J, Lee SM-Y, Yi C, Li C-W (2019) Controllable synthesis of functional nanoparticles by microfluidic platforms for biomedical applications-a review. Lab Chip 17(2):209–226

Ma J, Li CW (2018) Rapid and continuous parametric screening for the synthesis of gold nanocrystals with different morphologies using a microfluidic device. Sensor Actuat B-Chem 262:236–244

Nath N, Chilkoti A (2002) A colorimetric gold nanoparticle sensor to interrogate biomolecular interactions in real-time on a surface. Anal Chem 74:504–509

Navarro JRG, Manchon D, Lerouge F, Cottancin E, Lerme J, Bonnet C, Chaput F, Mosset A, Pellarin M, Parola S (2012) Synthesis, electron tomography and single-particle optical response of twisted gold nano-bipyramids. Nanotechnology 23:145707

Pappas TC, Wickramanyake WMS, Jan E, Motamedi M, Brodwick M, Kotov NA (2007) Nanoscale engineering of a cellular interface with semiconductor nanoparticle films for photoelectric stimulation of neurons. Nano Lett 7:513–519

Qi Y, Zhu J, Li J, Zhao J (2016) Highly improved synthesis of Au NBPs by tuning the concentration of hydrochloric acid. J Nanopart Res 18:190

Ren K, Zhou J, Wu H (2013) Materials for microfluidic chip fabrication. Accounts Chem Res 46:2396–2406

Sánchez-Iglesias A, Winckelmans N, Altantzis T, Bals S, Grzelczak M, Liz-Marzán LM (2016) High-yield seeded growth of monodisperse pentatwinned gold nanoparticles through thermally induced seed twinning. J Am Chem Soc 139:107–110

Thiele M, Soh JZE, Knauer A, Malsch D, Stranik O, Müller R, Csáki A, Henkel T, Michael Köhler JM, Fritzsche W (2016) Gold nanocubes-direct comparison of synthesis approaches reveals the need for a microfluidic synthesis setup for a high reproducibility. Chem Eng J 288:432–440

Uson L, Sebastian V, Arruebo M, Santamaria J (2016) Continuous microfluidic synthesis and functionalization of gold nanorods. Chem Eng J 285:286–292

Weissleder R, Nahrendorf M, Pittet MJ (2014) Imaging macrophages with nanoparticles. Nat mater 13:125–138

Whitesides GM (2006) The origins and the future of microfluidics. Nature 442:368